# Modeling of Human Welders' Operations in Virtual Reality Human–Robot Interaction

Qiyue Wang, Wenhua Jiao, Rui Yu, Michael T. Johnson, *Senior Member, IEEE*, and YuMing Zhang, *Senior Member, IEEE*

***Abstract*—This letter presents a virtual reality (VR) human–robot interaction welding system that allows human welders to manipulate a welding robot and undertake welding tasks naturally and intuitively via consumer-grade VR hardware (HTC Vive). In this system, human welders' operations are captured by motion-tracked handle controllers and used as commands to teleoperate a 6-DoF industrial robot (UR-5) and to request welding current from a controllable welding power supply (Liburdi Pulsweld P200). The three-dimensional (3-D) working scene is rendered in real time based on feedback information and shown to the human welder by head-mounted display via a motion-tracked headset. To compensate for the time delay between command motion and real motion of the robot, a hidden Markov model is proposed to model and predict human welders' operations. The K-means clustering algorithm is applied to cluster human welders' operation data (traveling speed) into latent states. Based on the developed prediction algorithm, the motion of human welders is predicted with an root mean square error (RMSE) accuracy of between 2.1 and 4.6 mm/s. The position data used as final commands to teleoperate a robot are predicted with an RMSE accuracy of between 1.1 and 2.3 mm. This letter presents a general cyber-physical model for human–robot interactive welding based on VR, building a foundation for welding robot teleoperation.**

***Index Terms*—Industrial robots, intelligent and flexible manufacturing, physical human-robot interaction, telerobotics and teleoperation, virtual reality and interfaces.**

## I. Introduction

ACCORDING to the International Federation of Robotics (IFR), over 50% of industrial robots are used for welding operations in the US and globally, including spot welding, arc welding, and laser welding [1], [2]. However, due to the difficulty of developing artificial intelligence (AI) based controls, currently most welding robots are pre-programmed through online teaching, off-line programming or a combination of the two [3], [4]. That is also why welding robots can be only applied to repeated welding tasks in a production line with strict requirements regarding a consistent working environment. To solve this problem, some welding process sensing, and control methods have been developed such as weld pool oscillation [5], [6], thermal sensing [7], and vision sensing [8], [9] to ensure welding quality across more variable working environments. However, due to the complexity of welding processes themselves (related to the complex thermal-mechanics-metallurgy reactions), process modeling and controlling are insufficient for practical applications. Compared with robots, skilled welding technicians can achieve steady and good welding quality regardless of working environment disturbance by adjusting welding parameters (welding current, travel speed etc.).

By taking advantage of the skills of welding technicians, three-level of applications have been proposed: (1) telerobotic welding [10], [11]: in which robots who have fewer physical limitations (temperature, pressure, vacuum, radiation) are used remotely as physical extensions of the human welders. This extends the human welders' working activity space significantly, such that unstructured welding tasks can be easily done in extreme environments (space, ocean, nuclear environment). (2) manual welding with robots assisting [12], [13]: human welders act together in the same welding process. With robotic assistance, tedious and strenuous manipulations for humans are lessened and sudden and abrupt motions which should be avoided in the welding process can be suppressed. This approach takes advantage of both human (high intelligence) and robots (high stability) to increase production efficiency and effectiveness. (3) welding robots demonstration-based imitation learning [14], [15]: in this approach, human welders work as masters to demonstrate their skills to robots as their apprentices. By recording state-action pairs, control policy characterizing human skills can be developed for the welding robots. After robots learn from human welders' demonstration, they can finish welding tasks independently. For all three above applications, information communication between human welders and robots plays a critical role. Many interfaces such as joysticks [16], [17], wearable sensors [18], gestures [19], and speech [20] have been proposed to transfer manipulation information from humans to robots. Onsite information (usually as visual information) are shown to the operator directly or via video stream in 2D or 3D display [21], [22]. With the recent rapid development of computer graphics, some customer-grade VR systems have been commercialized successfully such as Oculus Rift, HTC Vive, and PlayStation VR. By affording immersive and interactive ability, VR has been applied in prototype designing and skill training [23]–[26]. Compared

Manuscript received February 15, 2019; accepted May 28, 2019. Date of publication June 10, 2019; date of current version June 28, 2019. This letter was recommended for publication by Associate Editor C.-B. Yan and Editor J. Li upon evaluation of the reviewers' comments. *(Corresponding author: YuMing Zhang.)*

Q. Wang, W. Jiao, R. Yu, and Y. Zhang are with the Department of Electrical and Computer Engineering and the Institute for Sustainable Manufacturing, College of Engineering, University of Kentucky, Lexington, KY 40506 USA (e-mail: qiyue.wang@uky.edu; wenhua.jiao@uky.edu; rui.yu@uky.edu; yuming.zhang@uky.edu).

M. T. Johnson is with the Department of Electrical and Computer Engineering, University of Kentucky, Lexington, KY 40506 USA (e-mail: mike.johnson@uky.edu).

Digital Object Identifier 10.1109/LRA.2019.2921928

2377-3766 © 2019 IEEE. Personal use is permitted, but republication/redistribution requires IEEE permission.
See http://www.ieee.org/publications_standards/publications/rights/index.html for more information.

Authorized licensed use limited to: UNIVERSITY OF COLORADO. Downloaded on June 18,2020 at 18:37:15 UTC from IEEE Xplore. Restrictions apply.

with traditional computer aided design (CAD) methods, VR affords the immersive visualization and flexible feasibility evaluation for each component in product prototype designing stage and have been applied in the area of airplane [27], automotive [28], assembly tools [29] and house building [30], [31]. Skill training is another application of VR in industry to increase operation safety and reduce cost. Some VR-based training system have been developed in some common manufacture processes including welding [32], [33], painting [34] and mining [35]. In these training systems, a virtual environment is generated where the trainees can act and receive feedback about their operations. By interacting with virtual environment, the trainees learn the skills needed for real manufacture processes. Affording an intuitive and natural manipulation style is another advantage of VR system which is preferred to work as the interface between human and robots [36], [37]. In human-robot interaction (HRI), due to the response time of electromotors in robots, robots copy as the human operations but with delayed time. For some non-urgent tasks undertaken by robots such as pick-up and place and service [38], robots can use a "stop and wait" policy absorbing the time delay before completing tasks. However, for welding tasks, decisions may need to be applied immediately otherwise some weld defects may appear. Hence, a "stop and wait" policy cannot be applied in welding robots. Our proposed approach is to model and predict human welders' operations.

Human operations can be considered as a time-varying sequence, which researchers have proposed various methods to model. Dynamic time warping (DTW) is used to measure similarity and find the optimal match between two temporal sequences [39]. DTW can find a timing alignment even though the temporal sequences have different varying rates of motion relative to the template library [40], [41]. However, DTW cannot characterize the intrinsic randomness of human operation. Hence, some stochastic models have been used to model human motion. Gaussian mixture models (GMMs) [42], [43], hidden Markov models (HMMs) [41], [44] and conditional random fields (CRFs) [45] have been used for modeling human motion. Among these methods, HMM emphasizes the transition of latent state and has been widely used to model human motion. We choose an HMM to model human welders' operations due to the following three reasons: (1) The idea of transition between latent states can characterize the transition of human welders' perception to the welding process; (2) The idea of emission probability distribution can characterize the intrinsic uncertainty and randomness of human welders' operations. After modeling human welders' operations, a prediction algorithm is developed to predict human welders' future operations; (3) welding is an interactive process between human welders and welding scene including gap, arc, weld pool etc. This interaction of each human welder is unique and is an important criterion to evaluate human welders' skill. We would like to model the intrinsic characteristics of human welder operation without any external input information. HMM can be trained only using observed data sequence and apply for our application case perfectly.

This letter presents a virtual reality human-robot interactive welding system which is the first try to apply the VR system as interface between human welders and welding robots. The system configuration and working principle are presented which will enhance the foundation of human-robot interaction in welding area. What' more, this framework can be extend to other manufacture processes such additive manufacture and spraying. HMMs is also firstly applied to model the behavior of human welders considering the human welder operation characteristics including perception to working scene and time-sequence and randomness.

In Section II, the details of configuration, working principle and time delay of this virtual reality human-robot interaction welding system is presented. Section III talks about the principle of HMMs. Section IV introduces model parameters identification. Two prediction algorithms based on HMM and AR are developed in Section V. Verification results shows the prediction based on developed HMM has better performance. Finally, conclusions and future work are summarized in Section VI.

## II. System Configuration

### A. Hardware

The configuration of the developed cyber-physical system (CPS) model for human-robot interaction welding based on VR is shown in Fig. 1. In this system, a customer-grade VR system, HTC Vive, is used as the interface for human-robot interaction. HTC Vive comprises infrared cameras, motion-tracked handles and a headset. By combining capturing multi-markers positions with inertial measurement of handles and the headset, the motion of handles and the headset can be tracked with sub-millimeter accuracy in room-scale in real time (with 90 Hz fresh rate). The 3D virtual scene can be shown to human operators with head-mounted display (HMD). The robot is a 6-DoF collaborative industrial robot, UR-5, which has network interface and can be communicated with using TCP/IP protocol. A gas tungsten arc welding (GTAW) torch is installed in this robot and powered by Liburdi Pulsweld P200 welding supply which has computer interface and is designed for precise controllable welding. Welding is undertaken with direct current electrode negative (DCEN).

### B. Information Flow

As shown in Fig. 2, three objects communicate with each other in this cyber-physical system. A human welder takes the handle controller to do the operation $H$ captured by VR system and transmitted to a personal computer (PC) via APIs on Unity 3D, a popular game engine supporting almost all mainstream VR hardware. The operation information is separated into two parts after processing in the PC. One part is transmitted to the robot by local area network (LAN) as command pose $P_c$. The other part commands are welding current commands $C_c$ and are transmitted to the welding power supply by a data acquisition (DAQ) card using an analog input and output (AIO) function. At the same time, the pose of this robot $P_r$ and information about the welding process including the welding current and the voltage $C_r$ are transmitted back to the PC using the same LAN and DAQ card. In the PC, a 3D virtual working scene $E$ is rendered based on the information sensed from the actual

Authorized licensed use limited to: UNIVERSITY OF COLORADO. Downloaded on June 18,2020 at 18:37:15 UTC from IEEE Xplore. Restrictions apply.

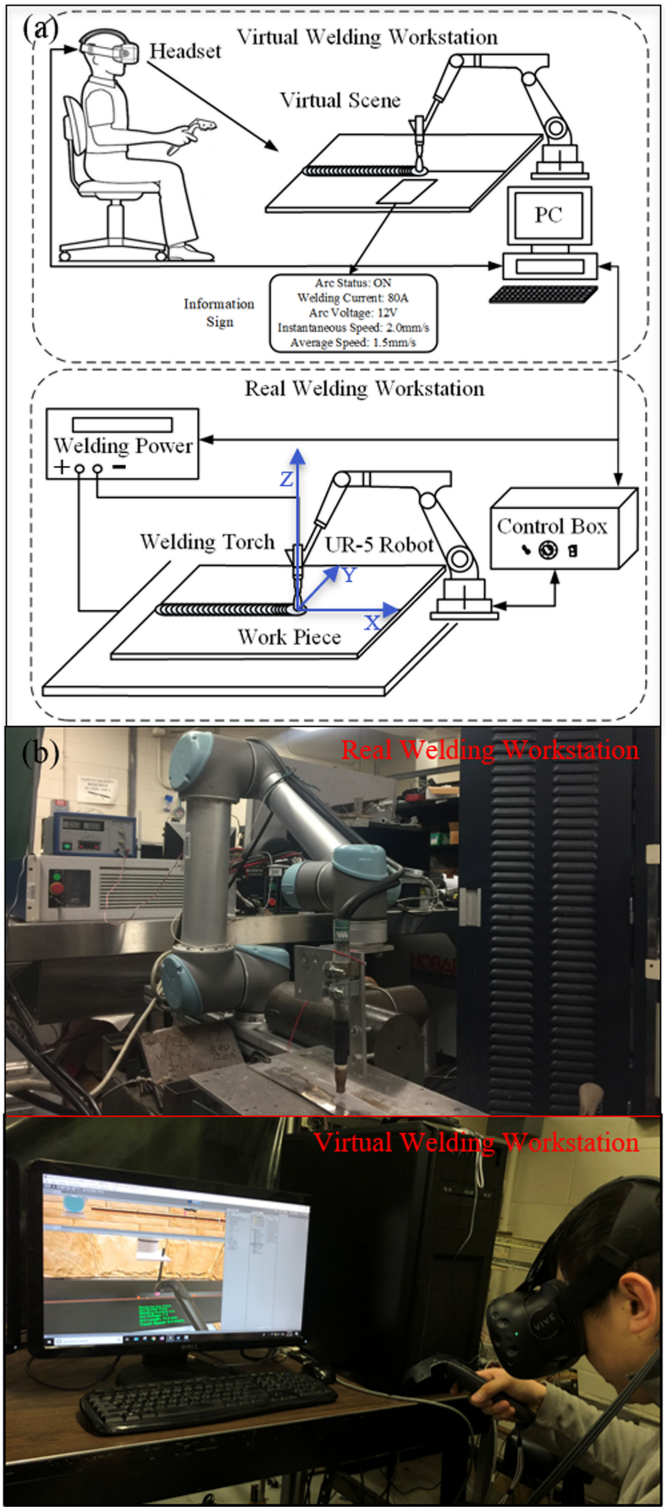


Fig. 1. Diagram for system configuration (a) schematic (b) practical.

welding environment and shown to the human welder via head-mounted display (HMD).

The developed virtual reality human-robot interactive welding system has following three unique advantages: (1) Spatial separability: human welders are separated with welding environment spatially by taking VR as the interface. Therefore, the harmful fume, gas and radiation are avoided to human welders; (2) Immersive ability: a 3D virtual and immersed working scene is generated, rendered and shown to human welders in real time which avoids missing on-site information due to spatial separation between human welders and working environment; (3) Operative ability: the control handles in VR afford a natural and intuitive operative style and make it possible to operate some innovative but heavy welding torches used in plasma welding and laser welding easily.

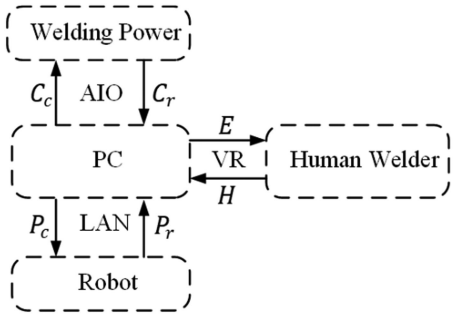


Fig. 2. Schematic diagram for information flow.

### C. Time Delay

If this virtual reality human-robot interaction system is an ideal teleoperation cyber-physical system (TCPS), the true pose of the robot should be the same as the command pose:

$$P_r = P_c \# \tag{1}$$

However, due to the existence of time delay and some movement error, the model can be modified as:

$$P_r(t) = P_c(t - \Delta t) + \xi(t) \# \tag{2}$$

where $\Delta t > 0$ characterizes the time delay and $\xi(t)$ is a noise signal assumed to be white noise: $\xi(t) = \xi$. Then $\Delta t$ is estimated such that:

$$\Delta t = \arg min_\tau \left( \|P_r(t) - P_c(t - \tau)\|_2 \right) \# \tag{3}$$

$$\|P_r(t) - P_c(t - \tau)\|_2 = \int_t (P_r(t) - P_c(t - \tau))^T (P_r(t) - P_c(t - \tau))\, dt \# \tag{4}$$

An artificial sinusoid-command is applied to identify the delayed time in x-axis which is shown in Fig. 3.

Using a variety of time shifts, the L2-norm of the difference between the command and the true pose is computed, as shown in Fig. 4. When $\tau = 0.5s$, we have:

$$\|P_r(t) - P_c(t - \tau)\|_2 = \min_\tau \left( \|P_r(t) - P_c(t - \tau)\|_2 \right) \# \tag{5}$$

Thus, the time delay is identified as $\Delta t = 0.5s$.

In order to make the robots track human welders' operations well with time delay. Prediction algorithm for human welders' operations is developed. The details are shown in Section III-V.

Authorized licensed use limited to: UNIVERSITY OF COLORADO. Downloaded on June 18,2020 at 18:37:15 UTC from IEEE Xplore. Restrictions apply.

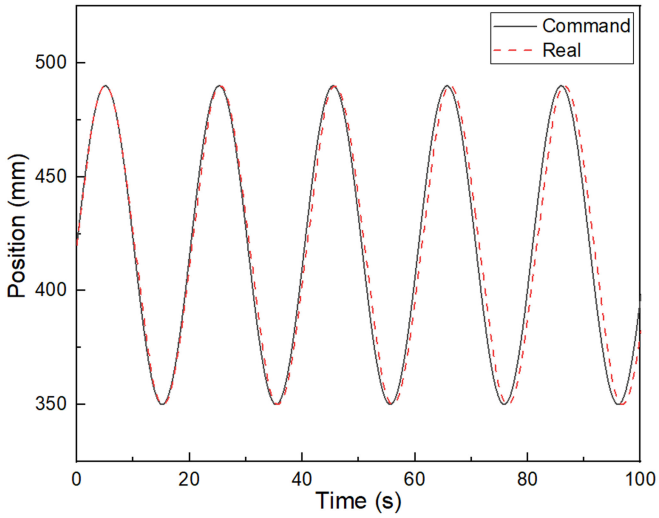


Fig. 3. Delay identification testing result.

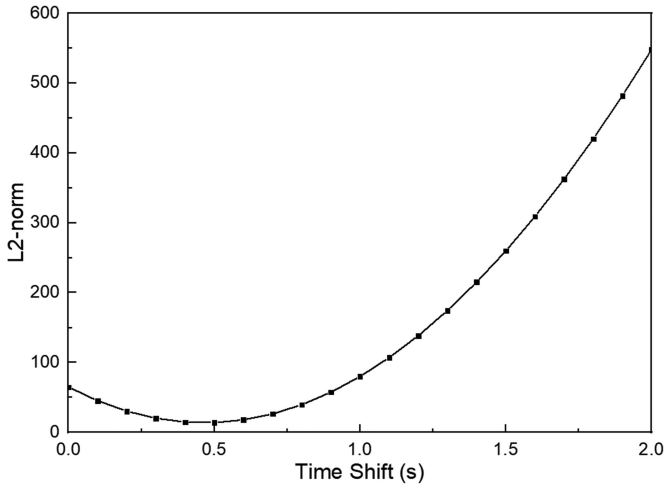


Fig. 4. L2-norm computation results with various time-shifts.

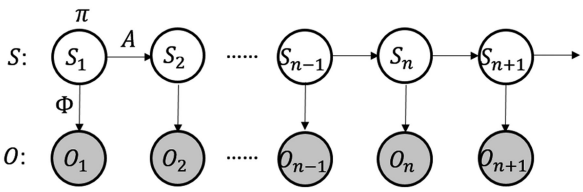


Fig. 5. Schematic diagram for an HMM.

## III. Principles of HMMS

HMMs are statistical models where latent states transfer as a Markov process and the observable variables depend on latent state. As shown in Fig. 5, in an HMM, $Q = \{q_1, q_2, q_3, \ldots, q_M\}$ is defined as a set of all possible states $q_i$. The instantaneous latent state $S$ transites among possible states of $Q$ with some probability $P(S_n|S_{n-1})$ characterized using the state transition matrix $A_{M\times M}$ where $A_{ij} \equiv P(S_n = q_j|S_{n-1} = q_i)$. Under each state, the observation variable $o$ has a probability distribution $P(o|q_i)$ called the emission probability distribution, characterized by the parameter $\Phi$. The initial state probability vector is $\pi = [\pi_1, \pi_2, \ldots, \pi_M]^T$ where $\pi_i = P(S_1 = q_i),\ i = 1, 2, \cdots M$. A complete HMM is determined by the a three-parameter set $\theta = \{A, \Phi, \pi\}$.

In the HMM developed here, human welders' intention is assumed to be stochastic and memoryless and have Markov property. Human manipulation velocity $v = [v_x, v_y, v_z]^T$ is taken as observed variables since travel speed is a key component of the GTAW process. Under each state $q_i$, we assume that the operation $o = v$ has a joint Gaussian distribution characterized by its mean value $u_i = \mu_{vi}$ and its covariance matrix $\Sigma_i$. The joint probability density function (PDF) of the human welders' operation can be written as:

$$P\left(o_i|q_i\right) = \frac{1}{2\pi\left|\Sigma_i\right|}\exp\left(-\frac{1}{2}(\mathrm{o}-u_i)^T{\Sigma_i}^{-1}\left(\mathrm{o}-u_i\right)\right)\# \tag{6}$$

## IV. Model Identification

### A. Latent State Identification

The latent states are hidden and not observable directly. In this HMM, observed data is the human manipulation velocity and can be clustered together due to the similarity if belonging to the same latent state. To accomplish this, K-means aiming to minimize inertia in equation (7) is applied to cluster observed data, with each cluster considered as a latent state. By trying different cluster number (k), the clustering result is shown in Fig. 6.

$$inertia = \sum_{i=0}^{n} \| x_i - u_j\|^2 \# \tag{7}$$

where $u_j$ is the centroid of $x_i$. When k $>$ 11, the inertia does not decrease greatly. Hence, k $=$ 11 is selected as the number of clusters and therefore the number of states. For each cluster of operation data, its cluster label is considered its state label. The cluster size distribution and clustering 2D visualization after principal component analysis (PCA) when k $=$ 11 are shown in Fig. 7.

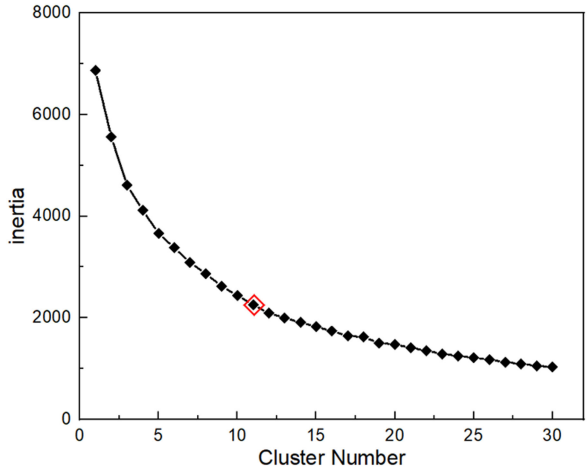


Fig. 6. Inertia value in K-means.

Authorized licensed use limited to: UNIVERSITY OF COLORADO. Downloaded on June 18,2020 at 18:37:15 UTC from IEEE Xplore. Restrictions apply.

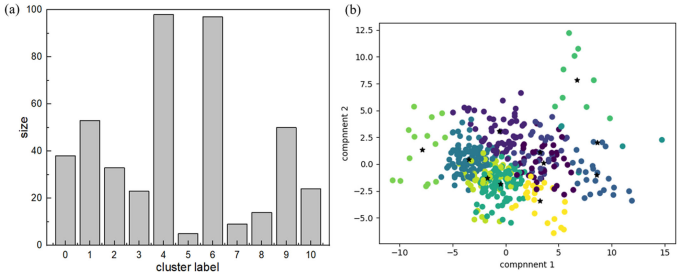


Fig. 7. Clustering results using K-means. (a) Cluster size distribution (b) 2D visualization after PCA.

### B. Model Parameter Identification

Based on this cluster model, the parameters of the HMM can be estimated as:

$$\begin{cases} \hat{A}_{ij} = \frac{N_{ij}}{\sum_{i=1}^{M} N_{ij}} \\ \hat{\mu}_i = \frac{\sum o_i}{N_i} \\ \hat{\Sigma}_i = \frac{\sum (o_i - \hat{\mu}_i)(o_i - \hat{\mu}_i)^T}{N_i - 1} \\ \hat{\pi}_i = \frac{T_i}{T} \end{cases} \# \tag{8}$$

where $N_{ij}$ is the number of pairs of observed data transitioning from state $i$ to state $j$ in one step;

$N_i$ is the number of observed data points whose state label is $i$;

$o_i$ is the observed data whose state label is $i$;

$T_i$ is the number of training sequences whose initial state label is $i$;

$T$ is the total number of training sequences;

Using human welders' operation data from the first author sampled with a rate of 2 Hz for one-step prediction purpose in section V, the parameters needed in developed HMM are identified by equation (8).

## V. Human Welders' Operations Prediction

The problem of predicting human welders' movement speed can be solved in three steps:

1) The current state based on current operation data can be estimated by:

$$P\left({s_i}^t | o^t\right) = \frac{P\left(o^t, {s_i}^t\right)}{\sum_{s_i} P\left(o^t, {s_i}^t\right)} \# \tag{9}$$

where

$$P\left(o^t, {s_i}^t\right) = P\left(o^t | {s_i}^t\right) * \sum_{s_j} P\left({s_i}^t | {s_j}^{t-1}\right) * P\left({s_j}^{t-1}\right) \# \tag{10}$$

2) Then the next state is estimated from the current state and transition matrix:

$$P\left({s_i}^{t+1}\right) = \sum_{s_j} P\left({s_i}^{t+1} | {s_j}^t\right) * P\left({s_j}^t\right) \# \tag{11}$$

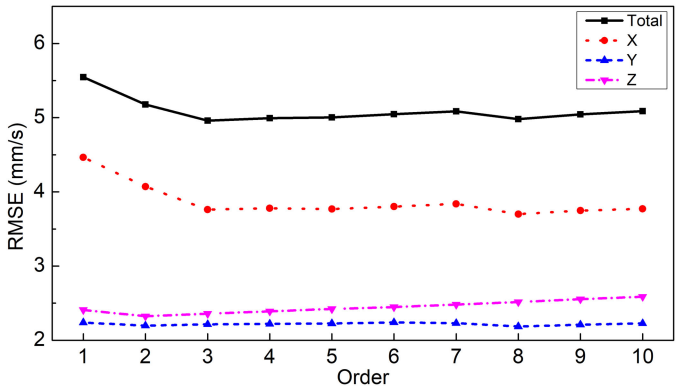


Fig. 8. Prediction error with different order in AR models.

TABLE I
Prediction Performance Comparation

| Model | Root Mean Square Error (mm/s) | | | |
|---|---|---|---|---|
| | *Speed_X* | *Speed_Y* | *Speed_Z* | *Speed_Total* |
| HMM | 3.330 | 2.118 | 2.374 | 4.606 |
| AR(3) | 3.761 | 2.215 | 2.358 | 4.961 |

3) Finally, the next operation estimation is estimated as the expectation of the observable data distribution for the next state:

$$\hat{o}^{t+1} = \sum_{s_i} P\left({s_i}^{t+1}\right) * u_i \# \tag{12}$$

For comparison, an alternative prediction model, autoregressive (AR) models in equation (13) with different order are also built to predict human welders' movements. The parameters $k_i$ is identified through least square regression.

$$\hat{o}^t = \sum_{i=1}^{n} k_i \cdot o^{t-i} \# \tag{13}$$

From Fig. 8, with the increasing of order in AR models, the performance is decreasing and remain a constant even increasing then due to overfitting. And the AR (3) model get the best overall performance of prediction accuracy with total RMSE as 4.961 mm/s. The prediction results using HMM and AR(3) are shown in Fig. 9 and the RMSE for the two models are computed and shown in Table I.

From Fig. 9 and Table I, the RSME of predicted total manipulation speed by HMM is decreased to 4.606 from 4.961 calculated from AR(3) model. In the x-axis and y-axis, we can see the significant improvement in prediction accuracy. In the z-axis, the HMM-based prediction accuracy is weaker than AR model. The reason is analyzed in following two aspects. (1) The proposed HMM makes a prediction for speed in 3 directions simultaneously whereas the AR model makes a prediction in each direction separately. In HMM based prediction, a weight is incorporated automatically based on the observed data covariance matrix. In our application, x-direction is the travel direction where the speed is larger than other two axis since movement

Authorized licensed use limited to: UNIVERSITY OF COLORADO. Downloaded on June 18,2020 at 18:37:15 UTC from IEEE Xplore. Restrictions apply.

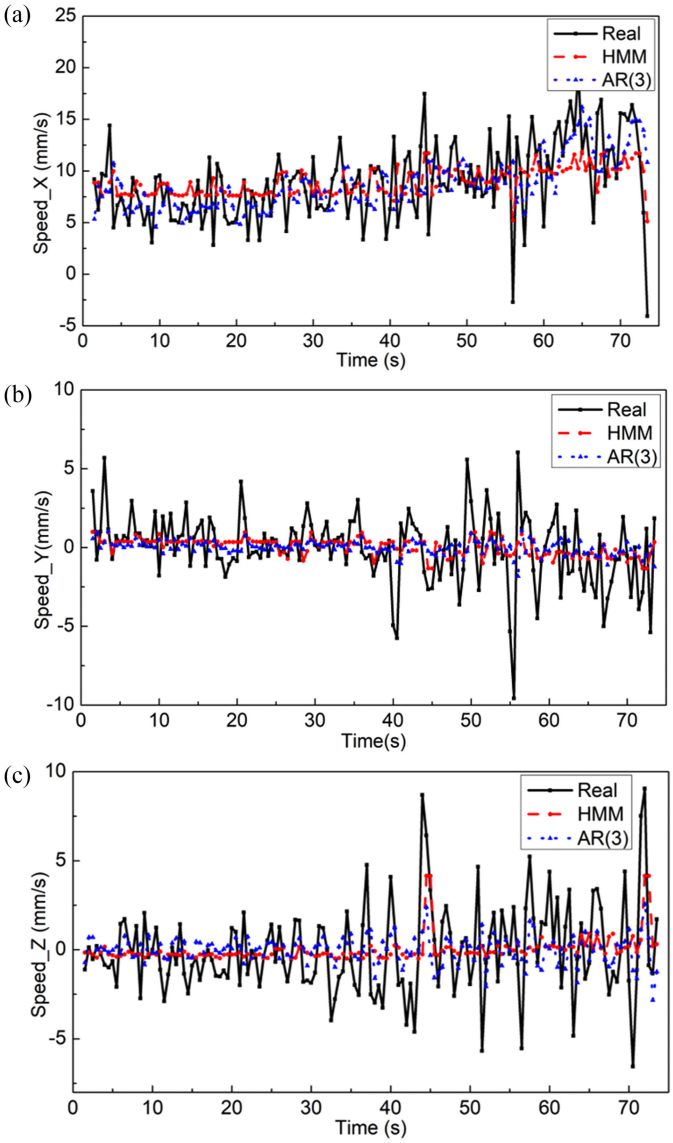


Fig. 9. Speed prediction (a) x-axis (b) y-axis (c) z-axis.

TABLE II
PREDICTION PERFORMANCE COMPARATION

| Root Mean Square Error (mm) | | | |
|---|---|---|---|
| *Postion_X* | *Position_Y* | *Position_Z* | *Position_Total* |
| 1.648 | 1.078 | 1.186 | 2.296 |

is primarily along the x-direction. This will cause some performance sacrifices in the other two directions, to maximize overall performance; (2) Due to the muscle structure, human is not good at control hand vertical shake comparing with horizonal movement. Therefore, the motion in z-axis is close to random value which is hard to predict.

In this virtual reality human-robot interaction welding system, position information is the final signal to command the robot. Hence, based on the predicted speed, position at the next time step is predicted as:

$$\hat{P}^{t+\Delta t} = P + \hat{v}^{t+\Delta t} * \Delta t\# \tag{14}$$

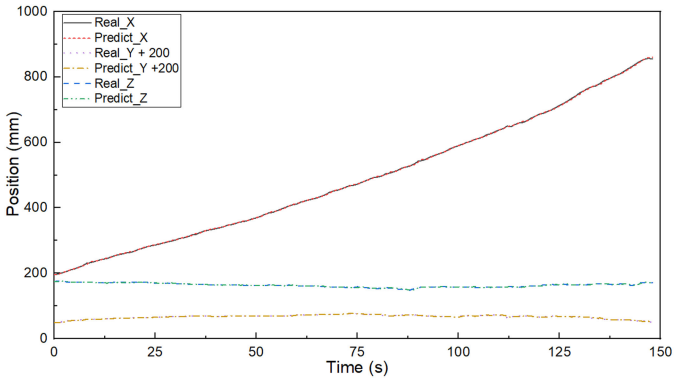


Fig. 10. Position prediction.

The resulting predictions based on this model are shown in Fig. 10 and Table II.

## VI. CONCLUSION AND FUTURE WORK

This letter introduces a cyber-physical system which allows human welders to implement welding tasks off-site. To achieve this goal, a human-robot interaction welding system based on VR is developed. A GTAW torch powered by a welding supply is installed in a 6-DoF UR-5 industrial robot. In order to immerse human welders in a 3D working scene, the HTC Vive is used as the interface between the human welders and a welding robot. The motion of the welders' hands is tracked by handle controllers in the VR system to manipulate the welding robot to accomplish welding tasks. The information about the working scene is sensed and used to generate an augmented 3D working scene shown to the welder via HMD. In order to compensate for the time delay in the system, a hidden Markov model is developed to characterize human welders' operational movements. A prediction algorithm is proposed to predict human welders' motion speed based on this HMM. Compared with an autoregressive model, the HMM shows better prediction performance.

This works has created a platform for human welders to teleoperate welding robots to undertake welding tasks intuitively and naturally. The modeling and prediction algorithm are tested in simple welding case where the weld seam is straight which is the most common, fundamental welding application such that we must address first. Further, we will explore other complex welding operations including 2D and 3D nonlinear trajectory and explore welding robot control policy learning from the demonstration of skilled welders.

## REFERENCES

[1] J. Sprovieri, "New technology for robotic welding," 2016. [Online]. Available: https://www.assemblymag.com/articles/93555-new-technology-for-robotic-welding
[2] G. Bekey and J. Yuh, "The status of robotics," *IEEE Robot. Autom. Mag.*, vol. 15, no. 1, pp. 80–86, Mar. 2008.
[3] Z. Pan, J. Polden, N. Larkin, S. Van Duin, and J. Norrish, "Recent progress on programming methods for industrial robots," in *Proc. 41st Int. Symp. Robot., ROBOTIK*, 2010, pp. 1–8.
[4] T. Brogårdh, "Present and future robot control development—An industrial perspective," *Annu. Rev. Control*, vol. 31, no. 1, pp. 69–79, 2007.

Authorized licensed use limited to: UNIVERSITY OF COLORADO. Downloaded on June 18,2020 at 18:37:15 UTC from IEEE Xplore. Restrictions apply.

[5] K. Andersen, G. E. Cook, R. J. Barnett, and A. M. Strauss, "Synchronous weld pool oscillation for monitoring and control," *IEEE Trans. Ind. Appl.*, vol. 33, no. 2, pp. 464–471, Apr. 1997.

[6] C. Li, Y. Shi, Y. Gu, and P. Yuan, "Monitoring weld pool oscillation using reflected laser pattern in gas tungsten arc welding," *J. Mater. Process. Technol.*, vol. 255, pp. 876–885, 2018.

[7] N. Chandrasekhar, M. Vasudevan, A. Bhaduri, and T. Jayakumar, "Intelligent modeling for estimating weld bead width and depth of penetration from infra-red thermal images of the weld pool," *J. Intell. Manuf.*, vol. 26, no. 1, pp. 59–71, 2015.

[8] Y. Liu and Y. Zhang, "Control of 3D weld pool surface," *Control Eng. Pract.*, vol. 21, no. 11, pp. 1469–1480, 2013.

[9] Y. Liu and Y. Zhang, "Model-based predictive control of weld penetration in gas tungsten arc welding," *IEEE Trans. Control Syst. Technol.*, vol. 22, no. 3, pp. 955–966, May 2014.

[10] H. Chao Li, H. Ming Gao, and L. Wu, "Teleteaching approach for sensor-based arc welding telerobotic system," *Ind. Robot.*, vol. 34, no. 5, pp. 423–429, 2007.

[11] Z. Liang, H. Gao, L. Nie, and L. Wu, "3D reconstruction for telerobotic welding," in *Proc. Int. Conf. Mechatron. Autom.*, 2007, pp. 475–479.

[12] M. S. Erden and B. Marić, "Assisting manual welding with robot," *Robot. Comput. Integr. Manuf.*, vol. 27, no. 4, pp. 818–828, 2011.

[13] M. S. Erden and A. Billard, "End-point impedance measurements at human hand during interactive manual welding with robot," in *Proc. IEEE Int. Conf. Robot. Autom.*, 2014, pp. 126–133.

[14] A. Hussein, M. M. Gaber, E. Elyan, and C. Jayne, "Imitation learning: A survey of learning methods," *ACM Comput. Surv.*, vol. 50, no. 2, pp. 21:1–21:35, 2017.

[15] W. Lawson, K. Sullivan, C. Narber, E. Bekele, and L. M. Hiatt, "Touch recognition and learning from demonstration (LfD) for collaborative human-robot firefighting teams," in *Proc. 25th IEEE Int. Symp. Robot Hum. Interactive Commun.,* 2016, pp. 994–999.

[16] S. K. Cho, H. Z. Jin, J. M. Lee, and B. Yao, "Teleoperation of a mobile robot using a force-reflection joystick with sensing mechanism of rotating magnetic field," *IEEE/ASME Trans. Mechatron.*, vol. 15, no. 1, pp. 17–26, Feb. 2010.

[17] E. M. Suero *et al.*, "Improving the human–robot interface for telemanipulated robotic long bone fracture reduction: Joystick device vs. haptic manipulator," *Int. J. Med. Robot. Assist. Surg*, vol. 14, no. 1, pp. 1863–1870, 2018.

[18] L.-H. Jhang, C. Santiago, and C.-S. Chiu, "Multi-sensor based glove control of an industrial mobile robot arm," in *Proc. Int. Automat. Control Conf.*, 2017, pp. 1–6.

[19] H. Liu and L. Wang, "Gesture recognition for human-robot collaboration: A review," *Int. J. Ind. Ergon.*, vol. 68, pp. 355–367, 2018.

[20] K. Zinchenko, C.-Y. Wu, and K.-T. Song, "A study on speech recognition control for a surgical robot," *IEEE Trans. Ind. Inform.*, vol. 13, no. 2, pp. 607–615, Apr. 2017.

[21] C. Yang, X. Wang, Z. Li, Y. Li, and C.-Y. Su, "Teleoperation control based on combination of wave variable and neural networks," *IEEE Trans. Syst., Man, Cybern., Syst.*, vol. 47, no. 8, pp. 2125–2136, Aug. 2017.

[22] H. Hedayati, M. Walker, and D. Szafir, "Improving collocated robot teleoperation with augmented reality," in *Proc. ACM/IEEE Int. Conf. Hum. Robot Interaction*, 2018, pp. 78–86.

[23] L. P. Berg and J. M. Vance, "Industry use of virtual reality in product design and manufacturing: A survey," *Virtual Reality*, vol. 21, no. 1, pp. 1–17, 2017.

[24] L. P. Berg and J. M. Vance, "An industry case study: Investigating early design decision making in virtual reality," *J. Comput. Inf. Sci. Eng.*, vol. 17, no. 1, 2017, Art. no. 011001.

[25] C. J. Turner, W. Hutabarat, J. Oyekan, and A. Tiwari, "Discrete event simulation and virtual reality use in industry: New opportunities and future trends," *IEEE Trans. Hum. Mach. Syst.*, vol. 46, no. 6, pp. 882–894, Dec. 2016.

[26] R. B. Hasan, F. B. A. Aziz, H. A. A. Mutaleb, and Z. Umar, "Virtual reality as an industrial training tool: A review," *J. Adv. Rev. Sci. Res.*, vol. 29, no. 1, pp. 20–26, 2017.

[27] C. Noon, R. Zhang, E. Winer, J. Oliver, B. Gilmore, and J. Duncan, "A system for rapid creation and assessment of conceptual large vehicle designs using immersive virtual reality," *Comput. Ind.*, vol. 63, no. 5, pp. 500–512, 2012.

[28] G. Lawson, P. Herriotts, L. Malcolm, K. Gabrecht, and S. Hermawati, "The use of virtual reality and physical tools in the development and validation of ease of entry and exit in passenger vehicles," *Appl. Ergon.*, vol. 48, pp. 240–251, 2015.

[29] A. Seth, J. M. Vance, and J. H. Oliver, "Virtual reality for assembly methods prototyping: A review," *Virtual Reality*, vol. 15, no. 1, pp. 5–20, 2011.

[30] A. Chellali, F. Jourdan, and C. Dumas, "VR4D: An immersive and collaborative experience to improve the interior design process," in *Proc. 5th Joint Virtual Reality Conf. EGVE EuroVR*, 2013, pp. 61–65.

[31] J. Whyte, N. Bouchlaghem, A. Thorpe, and R. McCaffer, "From CAD to virtual reality: Modelling approaches, data exchange and interactive 3D building design tools," *Autom. Construction*, vol. 10, no. 1, pp. 43–55, 2000.

[32] R. T. Stone, K. P. Watts, and P. Zhong, "Virtual reality integrated welder training," *Weld. J.*, vol. 90, no. 7, pp. 136s–141s, 2011.

[33] V. Bharath and R. Patil, "Solid modelling interaction with sensors in virtual environment for the application of virtual reality welding," in *Proc. Int. Conf. Current Trends Comput. Elect., Electron. Commun.*, 2017, pp. 645–647.

[34] G. A. Lee *et al.*, "Virtual reality content-based training for spray painting tasks in the shipbuilding industry," *ETRI J.*, vol. 32, no. 5, pp. 695–703, 2010.

[35] H. Zhang, "Head-mounted display-based intuitive virtual reality training system for the mining industry," *Int. J. Mining Sci. Technol.*, vol. 27, no. 4, pp. 717–722, 2017.

[36] E. Matsas and G.-C. Vosniakos, "Design of a virtual reality training system for human–robot collaboration in manufacturing tasks," *Int. J. Interactive Des. Manuf.*, vol. 11, no. 2, pp. 139–153, 2017.

[37] D. Whitney, E. Rosen, E. Phillips, G. Konidaris, and S. Tellex, "Comparing robot grasping teleoperation across desktop and virtual reality with ROS reality," in *Proc. Int. Symp. Robot. Res.*, Puerto Varas, Chile, Dec. 11–14, 2017.

[38] J. Gong, H. Wang, Z. Lu, N. Feng, and F. Hu, "Research on human-robot interaction security strategy of movement authorization for service robot based on people's attention monitoring," in *Proc. IEEE Int. Conf. Intell. Saf. Robot.*, 2018, pp. 521–526.

[39] D. J. Berndt and J. Clifford, "Using dynamic time warping to find patterns in time series," in *Proc. KDD*, 1994, pp. 359–370.

[40] S. Sempena, N. U. Maulidevi, and P. R. Aryan, "Human action recognition using dynamic time warping," in *Proc. Int. Conf. Elect. Eng. Inf.*, 2011, pp. 1–5.

[41] A. Vakanski, I. Mantegh, A. Irish, and F. Janabi-Sharifi, "Trajectory learning for robot programming by demonstration using hidden Markov model and dynamic time warping," *IEEE Trans. Syst., Man, Cybern., B*, vol. 42, no. 4, pp. 1039–1052, Aug. 2012.

[42] S. Chernova and M. Veloso, "Confidence-based policy learning from demonstration using gaussian mixture models," in *Proc. 6th Int. Joint Conf. Auton. Agents Multi-Agent Syst.*, 2007, Paper 233.

[43] S. M. Khansari-Zadeh and A. Billard, "Learning stable nonlinear dynamical systems with gaussian mixture models," *IEEE Trans. Robot.*, vol. 27, no. 5, pp. 943–957, Oct. 2011.

[44] J. Yang, Y. Xu, and C. S. Chen, "Hidden Markov model approach to skill learning and its application to telerobotics," *IEEE Trans. Robot. Autom.*, vol. 10, no. 5, pp. 621–631, Oct. 1994.

[45] A. Vakanski, F. Janabi-Sharifi, I. Mantegh, and A. Irish, "Trajectory learning based on conditional random fields for robot programming by demonstration," in *Proc. Robot. Application*, 2010, pp. 401–408.


Authorized licensed use limited to: UNIVERSITY OF COLORADO. Downloaded on June 18,2020 at 18:37:15 UTC from IEEE Xplore. Restrictions apply.